Grid Interactive Smart Buildings Coordination in Multi-Area Power Systems: A Delay-Robustness Analysis

Amedeo Andreotti[a], Bianca Caiazzo[b], Sara Leccese[c], Alberto Petrillo[d], Lorenzo Redi and Stefania Santini[e]

University of Naples Federico II, Italy

{amedeo.andreotti, bianca.caiazzo, sara.leccese, alberto.petrillo, lorenzo.redi, stefania.santini}@unina.it

Keywords: Distributed Control, Grid-Interactive Smart Buildings, Delay Robustness, Frequency Regulation, Demand Response.

Abstract: This work focuses on the frequency support control problem for Grid-Interactive Smart Buildings (GISBs) with Thermostatically-Controlled Loads (TCLs). The problem is formalized by leveraging multi-agent systems paradigm and a distributed delayed PID-based controller is introduced in order to guarantee that each GISB provides a fast frequency support to the main grid while maintaining a desired comfort level. Compared to the technical literature, the main novelty relies in considering communication latencies from the beginning of control design phase, thus guaranteeing that the proposed control protocol is able to counteract the unavoidable presence of heterogeneous time-varying delays arising during information sharing among all the electrical entities. Extensive simulation results, exploiting also latin hypercube sampling technique, show the effectiveness and the resilience of the approach with respect to delays and parameters uncertainties, while also highlighting the delay stability margin of the entire network.

1 INTRODUCTION

The rapid integration of Renewable Energy Sources (RESs), such as photovoltaic and wind power, has significantly changed the nature of power systems (Wang et al., 2019b; Duan et al., 2022). Although these greener resources promote a cleaner energy mix (Xia et al., 2019), they have also introduced crucial issues related to the stability of power systems. Indeed, their inherently variable and unpredictable nature can cause frequent and rapid power imbalances. Moreover, the high level of RESs spread has also significantly reduced system inertia by replacing synchronous machines (Zheng et al., 2021), thus increasing both the amplitude and the recurrence of frequency deviations (Zhao et al., 2023). It follows that, despite their crucial benefits devoted to greener and cleaner energy systems, RESs may compromise the overall grid reliability, thus requiring the need of *ad-hoc* countermeasures. (Wang et al., 2019b).

Paving the way towards innovative and adaptive strategies able to support frequency recovery while ensuring the stability of modern power systems is one of the fundamental issue to be addressed by researchers in the next years. In this direction, there is a growing interest into the usage of flexible resources from the demand side (Liu et al., 2022), such as Temperature-Controlled Loads (TCLs), i.e., heating, ventilation and air-conditioning systems able to quickly respond to power system variations (Xiao et al., 2023). Unlike traditional demand response systems, which often disrupt user activities, TCLs can also provide grid support while maintaining at the same time a proper comfort level by means of predefined temperature ranges. The recent trend is the evaluation of collective effects provided by a multiple aggregated TCLs, which leads to the so-called Grid-Interactive Smart Buildings (GISBs) paradigm. Specifically, GISBs represent an aggregation of TCLs, which can be viewed as one single entity from grid perspective able to act as virtual energy storage and provide timely support to frequency regulation (Wang et al., 2019b; Wang et al., 2019a).

Centralized solutions have been widely explored to address coordination control problem of TCLs (Zhang et al., 2018; Zhao et al., 2016). How-

[a] https://orcid.org/0000-0002-6514-6807
[b] https://orcid.org/0000-0002-1676-2814
[c] https://orcid.org/0009-0001-8939-1129
[d] https://orcid.org/0000-0003-4630-6673
[e] https://orcid.org/0000-0002-0754-6271

Andreotti, A., Caiazzo, B., Leccese, S., Petrillo, A., Redi, L. and Santini, S.
Grid Interactive Smart Buildings Coordination in Multi-Area Power Systems: A Delay-Robustness Analysis.
DOI: 10.5220/0013357600003953

In *Proceedings of the 14th International Conference on Smart Cities and Green ICT Systems (SMARTGREENS 2025)*, pages 48-55
ISBN: 978-989-758-751-1; ISSN: 2184-4968

ever, these architectures face some limitations, especially related to scalability issue and high computational burdens, which become more crucial as far as the number of spatially distributed systems increases. That's way latest GISB control strategies are moving towards distributed control solutions, which exploit Multi-Agent Systems (MASs) modeling approach to deal with the coordination of multiple TCLs. In this perspective, each spatially distributed building is modeled as an agent able to share its own local information with the corresponding neighboring set by means of a communication network in order to achieve a global coordinated behavior (Ge et al., 2018). Along this line, a distributed average consensus algorithm has been introduced in (Chen et al., 2014) to solve the fair power allocation problem in a TLC aggregator. Authors in (Zheng et al., 2021) have proposed a distributed control approach for frequency support in aggregated buildings able to balance their energy level while guaranteeing robust and reliable operations with a desired comfort level for the occupants. Moreover, in (Wang et al., 2019a) a two-layer distributed control protocol accounting for both the inner and the inter buildings communication graphs has been designed. Furthermore, in (Wang et al., 2019b), by the means of double layer control protocols, authors achieve both fair power allocation among GISBs and a proper comfort level among all available TCLs. These control objectives are fulfilled by means of a distributed sliding mode controller, which provides also robustness and fast response under varying conditions.

Besides the benefits of distributed control approaches, the control over communication networks poses several challenges. Since the information exchange among buildings is realized via a wireless communication network, random delays usually arise. In this context, each GISB receives information with different time-varying delays, whose value depends on the network conditions and the specific communication channel. It follows that delays may significantly affect the aggregator control performance and compromise frequency support capability. Furthermore, in the worst case, delays may lead to the instability of the overall network (Caiazzo et al., 2022). Based on the above, one can conclude that delays should be considered from the beginning in order to prevent dangerous and undesirable situations, i.e., from the control design phase. This implies that the distributed controller has to be designed and implemented via outdated information, which can be done by using the time stamp inserted into messages to correctly correlate the information.

Based on the these considerations, this article aims at designing a distributed controller for the coordination of a GISBs aggregator able to provide fast frequency support to the grid in normal operating conditions despite the presence of unavoidable communication delays. We would like to highlight that, compared with (Wang et al., 2019b), where the simulation campaign has also involved a robustness analysis with respect to constant and homogeneous communication delay, here we allow delays to be time-varying and heterogeneous for each electrical entity within the network, while considering them from the control design phase. We carry out an extensive simulation campaign in order to derive the delay stability margin, i.e., the maximum tolerable delay preserving the stability of the the overall power system. Moreover, to further confirm the effectiveness of the proposed approach, we also employ the Latin Hypercube Sampling (LHS) method to assess the control performance under several parameters and communication delays uncertainties/variations, as well as for all the possible combinations of them.

Finally, the paper structure is given as follows. In Section 2 the problem statement is detailed along with the modeling of the multi-area power system. The distributed control protocol for frequency support problem with heterogeneous time-varying delays is presented in Section 3, while simulation results are reported in Section 4. Conclusions are drawn in Section 5.

2 PROBLEM FORMULATION

Consider a multi-area power system composed by M control areas physically interconnected through tie-lines. Each area k ($k = 1, \cdots, M$) consists of variable local loads and N_k GISBs. These latter are equipped with only air conditioning systems and share their temperature information with the corresponding neighboring GISBs via a wireless communication network subject to communication impairments. Thus, the N_k GISBs in the k-the area act as a single aggregator for the fast frequency support of the multi-area power system.

Inspired by (Wang et al., 2019b), the aim of this work is to design a novel distributed controller for the GISBs able to guarantee that the whole aggregator provides a fast frequency support to the main grid −while maintaining its temperature within user-defined ranges− despite the presence of communication latencies.

In the sequel we firstly provide the modeling of the multi-area power system we consider herein.

2.1 Network Modeling

The communication among GISBs into the k-the control area can be modeled as a directed graph $\mathcal{G}^c_{N_k} = \{\mathcal{V}^c_{N_k}, \mathcal{E}^c_{N_k}, \mathcal{A}^c_k\}$, where $\mathcal{V}^c_{N_k}$ is the set of the N_k GISBs and $\mathcal{E}^c_N \subseteq \mathcal{V}^c_N \times \mathcal{V}^c_N$ stands for the edges set describing the active communication links. Matrix $\mathcal{A}^c_k = [a^k_{ij}] \in \mathbb{R}^{N_k \times N_k}$ is the adjacency matrix, whose elements are $a^k_{ij} = 1$ if there exists a link between the i-th and j-th GISBs, 0 otherwise. Associated to this graph there is the Laplacian matrix $\mathcal{L}_k = [l^k_{ij}] \in \mathbb{R}^{N_k \times N_k}$ such that $l^k_{ii} = \sum_{j=1}^{N_k} a^k_{ij}$ and $l^k_{ij} = -a^k_{ij}$, $j \neq i$. Since we assume also the presence of a virtual building into the cyber-space imposing the reference behavior to the specific k-th control area, it results an augmented directed graph $\mathcal{G}^c_{N_k+1}$ with a Pinning matrix $\mathcal{P}_k = diag\{p^k_1, p^k_2, \dots, p^k_{N_k}\}$, whose elements are such that $p^k_i = 1$ if the leader GISB is directly connected to the i-th GISB, $p^k_i = 0$ otherwise. Finally, the set of neighbors of the i-th GISB is defined as $\mathcal{N}^c_{i,k} = \{j : (i, j) \in \mathcal{E}^c_{N_k+1}\}$.
The overall electric topology of the multi-area power system can be also modeled as a connected weighted graph $\mathcal{G}^e_N = \{\mathcal{V}^e_N, \mathcal{E}^e_N, T\}$, where $\mathcal{V}^e_N$ is the set of electrical buses connecting the different control areas, while $\mathcal{E}^e_N$ represents the set of electric power lines. Furthermore, T is the associated weighted adjacency matrix, whose elements are such that $T_{k,\iota} = 1$ if and only if there is a tie-line between the area k and area ι, $T_{k,\iota} = 0$ otherwise, for any $k, \iota \in \{1, \cdots, M\}$.

2.2 Multi-Area Power System Model

Here we firstly detail the model of the entire multi-area power system by means of Load Frequency Control (LFC) and, then, we move towards the description of the single GISBs dynamics.

2.2.1 Load Frequency Control

The stability of the overall power system is ensured via LFC (Wadi et al., 2024), whose objective is to guarantee that the frequency deviations remain within an allowable ranges, despite the presence of additional loads (Yousef et al., 2014). The typical LFC structure within the single area, reported in Figure 1, allows the physical connection with other different control areas, thus automatically balancing and sharing the load among them. Beside the LFC, we assume that the power output of the generators is controlled by their primary and secondary controllers (Wang et al., 2019b). The relation between power mismatch and frequency deviation into the k-th area can be modeled as

$$\Delta f_k(s) = \frac{1}{2H_k s + D_k}\Bigg(-\Delta P^L_k(s) + \Delta P^{RES}_k(s) + M_k(s)\Big(\Delta P^c_k(s) - \frac{1}{R^G_k}\Delta f_k(s)\Big) - \Delta P^{tie}_k(s) + \Delta P^{agg}_k(s)\Bigg), \quad (1)$$

where Δf_k is the frequency deviation in the k-th control area, H_k and D_k are the load damping and the inertia of the system, respectively, while R_k stands for the speed droop coefficient. Furthermore, ΔP^c_k is the secondary control input, while ΔP^L_k, ΔP^{RES}_k, ΔP^{tie}_k and ΔP^{agg}_k are the power variations of loads, RESs, tie-line and GISBs aggregator, respectively. M_k denotes the generators dynamics, which can be expressed as

$$M_k(s) = \frac{1}{1 + sT^G_k} \cdot \frac{1}{1 + sT^T_k} \cdot \frac{1 + sT^{CA}_k}{1 + sT^{CB}_k}, \quad (2)$$

where T^G_k and T^T_k are the time constants of the generator and turbine, respectively, while T^{CA}_k and T^{CB}_k are the time constants of the transient droop compensator (Wang et al., 2019b).
The power transfer between the k-th and the ι-th control areas, $k, \iota, \in \{1, \dots, M\}$, is computed as

$$\Delta P^{tie}_k(s) = \frac{2\pi}{s}\left(\sum_{\iota=1}^{M} T_{k\iota}(\Delta f_k(s) - \Delta f_\iota(s))\right). \quad (3)$$

According to the technical literature (Wu et al., 2017), the secondary control input ΔP^c_k in (1) is usually designed as a PI controller weighing the current value of the Area Control Error (ACE), whose expression is derived as

$$ACE_k(s) = B_k \Delta f_k(s) + \Delta P^{tie}_k(s), \quad (4)$$

where B_k is the frequency bias factor of the k-th control area. Hence, by defining K_p and K_i as the proportional and integral gains respectively, the PI-based secondary controller is provided as follows:

$$\Delta P^c_k(s) = \Big(K_p + \frac{K_i}{s}\Big) ACE_k(s). \quad (5)$$

However, fast frequency recovery cannot be ensured by means of the solely secondary control input (5) (Wang et al., 2019b). Hence, our aim is to adjust the value of the total power required by the smart buildings aggregator, i.e., $\Delta P^{agg}_k(s)$ in (1), so to make the frequency recovery faster, which is not possible by means of (5).

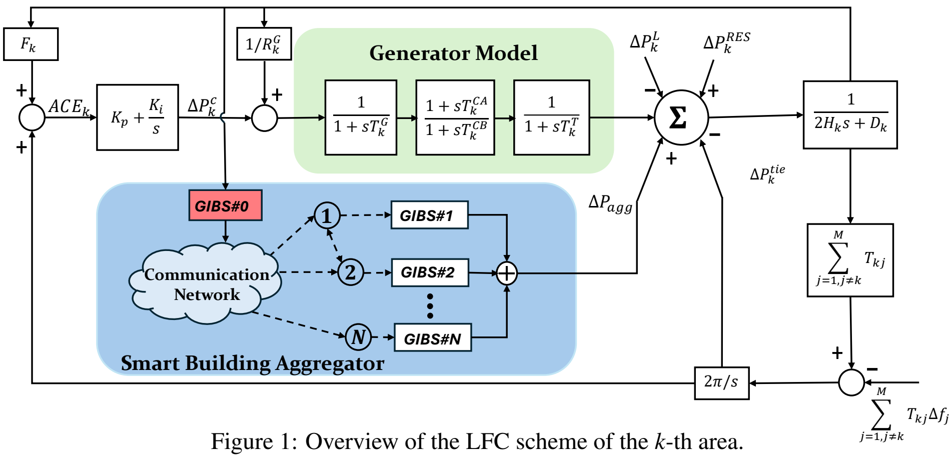

Figure 1: Overview of the LFC scheme of the k-th area.

2.2.2 Smart Buildings Thermal Dynamic Model

Through this work we assume the i-th smart building into the k-th area to be equipped with only TCLs, thus implying that its dynamical behavior can be modeled by means of its average temperature, i.e., (Wang et al., 2019b):

$$C^{th}_{i,k}\dot{\theta}_{i,k}(t) = \frac{\theta_{amb,k}(t) - \theta_{i,k}(t)}{R^{th}_{i,k}} - \eta_{i,k}\frac{p_{i,k}(t)}{\lambda_{i,k}} + \omega_{i,k}(t), \tag{6}$$

where $\theta_{i,k}(t)$ and $\theta_{amb,k}(t)$ are the internal and ambient temperatures, $C^{th}_{i,k}$ and $R^{th}_{i,k}$ are the thermal capacitance and resistance, respectively, $\lambda_{i,k}$ is the number of TCLs in the i-th building, $p_{i,k}(t)$ represents the power consumption. Furthermore, $\eta_{i,k}$ is the thermal coefficient which is defined as $\eta_{i,k} > 0$ for cooling TLC and $\eta_{i,k} \leq 0$ for heating ones. Finally, $\omega_{i,k}(t)$ represents a Gaussian disturbance with zero means.
However, in practical applications a GISB has to keep its temperature within a user-defined range, which may differ between different buildings. Hence, by defining this temperature range as $[\bar{\theta}_{i,k} - \Delta\theta_{i,k},\ \bar{\theta}_{i,k} + \Delta\theta_{i,k}]$, with $\bar{\theta}_{i,k}$ and $\Delta\theta_{i,k}$ the set-point temperature and its admissible tolerance, we can introduce an additional variable $\varepsilon_{i,k}(t) \in [0,1]$ standing for the comfort level index, i.e.:

$$\varepsilon_{i,k}(t) = \frac{\theta_{i,k}(t) - \bar{\theta}_{i,k} + \Delta\theta_{i,k}}{2\Delta\theta_{i,k}}. \tag{7}$$

Then, by substituting this latter into (6) and defining the time-varying disturbance $d_{i,k}(t) = \frac{\theta_{amb,k}(t) - \bar{\theta}_{i,k} + \Delta\theta_{i,k} + R^{th}_{i,k}\omega_{i,k}}{2\Delta\theta_i C^{th}_{i,k} R^{th}_{i,k}}$, we obtain:

$$\dot{\varepsilon}_{i,k}(t) = \frac{1}{C^{th}_{i,k}R^{th}_{i,k}}\varepsilon_{i,k}(t) - \frac{\eta_{i,k}}{2\Delta\theta_{i,k}C^{th}_{i,k}\lambda_i}p_{i,k}(t) + d_{i,k}(t). \tag{8}$$

Note that, the comfort level reflects the thermal power of the i-th building. Specifically, whenever the i-th GISB reaches its maximum allowable temperature, then $\varepsilon_{i,k}(t) = 1$, meaning that the cooling capacity of its own TLC cannot be further reduced. On the other hand, if the comfort level of the i-th GISB is such that $\varepsilon_{i,k}(t) = 0$, it means that it is working at its minimum allowable temperature and, hence, its cooling capacity cannot be further increased (Wang et al., 2019b). Following (Wang et al., 2019b), we introduce an auxiliary state variable $\zeta_{i,k}(t)$, whose expression is given as follows:

$$\zeta_{i,k}(t) = a_{i,k}\varepsilon_{i,k}(t) + b_{i,k}p_{i,k}(t) + d_{i,k}(t), \tag{9}$$

being $a_{i,k} = \frac{1}{C^{th}_{i,k}R^{th}_{i,k}}$ and $b_{i,k} = \frac{\eta_i}{2\Delta\theta_{i,k}C^{th}_{i,k}\lambda_{i,k}}$. Then, the comfort level dynamics of the i-th building can be recast as a control-oriented state-space model, i.e.:

$$\dot{x}_{i,k}(t) = A_{i,k}x_{i,k}(t) + B_{i,k}(u_{i,k}(t) + d_{i,k}(t)), \tag{10}$$

where $x_{i,k}(t) = [\varepsilon_{i,k}(t),\ \zeta_{i,k}(t)]^\top$, $u_{i,k}(t) = \dot{p}_{i,k}(t)$ is the distributed control input to be designed, while $A_{i,k}$ and $B_{i,k}$ are defined as:

$$A_{i,k} = \begin{bmatrix} 0 & 1 \\ 0 & a_{i,k} \end{bmatrix}, \quad B_{i,k} = \begin{bmatrix} 0 \\ b_{i,k} \end{bmatrix}. \tag{11}$$

The amount of power that each building within the aggregator has to consume to maintain its comfort level at a constant reference value $\bar{\varepsilon}_{0,k}$ is defined as *baseline* power $p^k_{b,i}(t)$, which can be computed as

$$p^k_{b,i}(t) = \lim_{t\to\infty}\frac{-a_{i,k}\bar{\varepsilon}_k - d_{i,k}(t)}{b_{i,k}}. \tag{12}$$

Thus, the baseline power of the k-th GISBs aggregator is $P^k_b(t) = \sum_{i=1}^{N_k} p^k_{b,i}(t)$, $k \in \{1,\ldots,M\}$.

Remark 1. *Similar to an energy storage system with dissipation, a GISB maintains its desired temperature while operating at baseline power. Indeed, when its power consumption is less then the baseline $P^k_b(t)$, it injects power (i.e., discharges) into the grid, whereas* *whenever its power consumption increases w.r.t. the baseline, it is able to absorb power (i.e., charge) from the grid (Wang et al., 2019b). Hence, by controlling the GISBs aggregator power consumption, i.e. the reference comfort level, the frequency deviation of the k-th area can be stabilized.*

The control problem addressed through this manuscript can be formulated as follows.

Problem 1. *Consider an energy community of M control areas physically interconnected via tie-lines, each of them composed of N_{k+1} GISBs sharing information via a communication network. Design a distributed control law able to ensure that all GISBs within the k-th area, $k \in \{1,\dots,M\}$, are able to track the reference behaviour imposed by the corresponding leader $x_{0,k}(t) = [\varepsilon_{0,k}(t),\ \zeta_{0,k}(t)]^\top$. This problem can be mathematically recast as a leader-tracking consensus, whose control objective is to find $u_{i,k}(t)$ in* (10) *such that, $\forall i = 1,\cdots,N_k$,*

$$\lim_{t\to\infty} \|x_{0,k}(t) - x_{i,k}(t)\| = 0, \quad k \in \{1,\dots,M\}, \tag{13}$$

despite the presence of unavoidable communications delays.

3 DISTRIBUTED FREQUENCY SUPPORT CONTROL WITH HETEROGENEOUS TIME-VARYING DELAYS

Before presenting the distributed control protocol we propose through this work, we firstly detail the leader behavior within each control area according to the technical literature (Wang et al., 2019b).

3.1 Leader Control

To solve Problem 1, we assume that, in each area k, the reference comfort level is provided by a virtual GISB, labeled with index 0, i.e., $x_{0,k}(t)$, whose behavior is derived according to (Wang et al., 2019b). Specifically, based on grid frequency conditions, it operates in two distinct modes, i.e., *i*) Frequency Support Mode (FSM) and *ii*) Comfort Recovery Mode (CRM). For sake of clarity, in what follows we provide a description of both operating modalities.

Frequency Support Mode. FSM is activated whenever the system frequency deviations exceed a predefined threshold which denotes a critical imbalance between power generation and consumption. Under these conditions, the k-th GISB aggregator provides a primary frequency support by dynamically adjusting its power consumption, which can be computed as

$$\begin{aligned} P_k(t) &= \sum_{i=1}^{N_k} p_{i,k}(t) \\ &= \begin{cases} P_b^k(t) + R^{agg,k}(\Delta f_M - \Delta f_k(t)), & \Delta f_k \geq \Delta f_M, \\ P_b^k(t) + R^{agg,k}(\Delta f_m - \Delta f_k(t)), & \Delta f_k \leq \Delta f_m, \end{cases} \end{aligned} \tag{14}$$

where $R^{agg,k}$ is the droop gain of the k-th GISB aggregator, while Δf_M and Δf_m stand for the maximum and the minimum acceptable frequency values. These latter are usually equal to $\Delta f_M = 0.1\,[Hz]$ and $\Delta f_m = -0.1\,[Hz]$ (Wadi et al., 2024). By virtue of (14), the k-th leader is able to discharge (charge) power to (from) the grid during frequency drops (surpluses). In this operational mode, based on (9) and (14), the behavior of the k-th leader is described as follows:

$$\begin{cases} \varepsilon_{0,k}(t) = \int_0^t \zeta_{0,k}(t)dt \\ \zeta_{0,k}(t) = \frac{\sum_{i=1}^{N_k} b_{i,k}p_{i,k}(t) + \sum_{i=1}^{N_k}[a_{i,k}\varepsilon_{i,k}(t) + d_{i,k}(t)]}{N_k}, & \forall k. \end{cases} \tag{15}$$

Comfort Recovery Mode. We say that the k-th GISBs aggregator operates in CRM mode whenever $\Delta f_k \in [\Delta f_m,\ \Delta f_M]$. In this case, the temperature of each smart building involved into the single area control is kept at a certain value and, hence, the whole aggregator absorbs an amount of power that is $P_b^k(t)$. Thus, the leader behavior $x_{0,k}(t) = cost$ with $\varepsilon_{0,k}(t) = \bar{\varepsilon}_{0,k}$ and $\zeta_{0,k}(t) = 0$.

Based on these two operational modes, we finish-up into a double-layer control architecture for each control area as in (Wang et al., 2019b), with the first layer provided by the leader behavior and the second layer to be designed to satisfy objective (13) in Problem 1.

3.2 Cooperative Control Protocol for the GIBS

Here, the objective is to handle Problem 1 arising in each control area, i.e., to guarantee that all GISB within the k-th area, $k \in \{1,\dots,M\}$, track the corresponding leader behavior $x_{0,k}(t)$. Furthermore, the distributed control strategy we aim to design has to counteract the presence of time-varying communication delays arising during information sharing process. For each building i, $i = 1,\cdots,N_k$, $k = 1,\dots,M$, we firstly define the error with respect to the corresponding leader as:

$$e_{i,k}(t) = \begin{bmatrix} e_{\varepsilon,i,k}(t) \\ e_{\zeta,i,k}(t) \end{bmatrix} = \begin{bmatrix} \varepsilon_{i,k}(t) - \varepsilon_{0,k}(t) \\ \zeta_{i,k}(t) - \zeta_{0,k}(t) \end{bmatrix}. \tag{16}$$

To deal with Problem 1 we propose the following distributed networked PID-based delayed control strategy:

$$
\begin{aligned}
u_{i,k}(t,\tau^k_{i,k}(t)) = &\\
&+k_p \sum_{j\in\mathcal{N}_i^c} a^k_{ij}(e_{i,k}(t-\tau^k_{i,k}(t)) - e_{j,k}(t-\tau^k_{i,k}(t)))\\
&+k_d \sum_{j\in\mathcal{N}_i^c} a^k_{ij}(\dot{e}_{i,k}(t-\tau^k_{i,k}(t)) - \dot{e}_{j,k}(t-\tau^k_{i,k}(t))),\\
&+k_i \sum_{j\in\mathcal{N}_i^c} a^k_{ij}\int_0^t (e_{i,k}(s-\tau^k_{i,k}(s)) - e_{j,k}(s-\tau^k_{i,k}(s)))\,ds,
\end{aligned}
\tag{17}
$$

where k_p, k_d, k_i are the proportional, derivative and integral control gains, respectively, while a^k_{ij} models the communication network topology into the k-th control area emerging from the presence/absence of the communication link between i-th and j-th GISB (see Section 2.1). Furthermore, $\tau^k_{ij}(t)$ represents the communication time-varying delays between the i-th and j-th GISB, for all $i,j \in \mathcal{V}^c_{N_k}$, which is assumed to be detectable by timestamp. In doing so, (17) is computed via outdated information, thus preventing any instability phenomena (Caiazzo et al., 2022).

Assumption 1. *(Andreotti et al., 2021) Time-varying time-delays signals $\tau^k_{ij}(t)$ are bounded and slowly-varying, i.e., $\tau^k_{ij}(t) \leq \tau^\star$ and $\dot{\tau}^k_{ij}(t) \leq \mu < 1$, $\forall i,j \in \mathcal{V}^c_{N_k}, \forall k \in \{1,\cdots,M\}$.*

Remark 2. *The stability of the* (10) *under the action of* (17) *can be proved by means of Lyapunov-Krasovskii theory for time-delay systems (see, e.g., (Andreotti et al., 2021)).*

4 NUMERICAL ANALYSIS

In this section we validate the effectiveness of the proposed control (17) in coordinating GISBs aggregator for fast frequency support despite the presence of heterogeneous time-varying communication delays. To this aim, we leverage MATLAB/Simulink simulation platform to emulate a multi-area power system consisting of $M = 2$ control areas, each of them including an aggregator of $N_k = 12$ buildings, $k = 1,2$. Without loss of generality, the LFC parameters in (1) are assumed to be equal in both control areas and all the buildings have the same physical characteristics. Communication and electrical topologies are chosen according to Figure 2, while multi-area system parameters are chosen according to (Wang et al., 2019b). From these latter, we have $a_{i,k} = -0.25$, $b_{i,k} = -3.125\times10^{-3}$, $d_{i,k} = 0.5625$, $\lambda_{i,k} = 100$, for all $i \in \mathcal{V}^c_{N_k}$, $k = 1,2$. The initial reference comfort level in each control area provided by the corresponding virtual GISB during CRM is set as

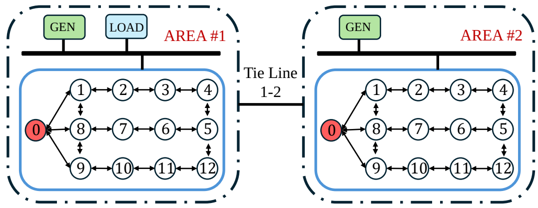

Figure 2: Communication and electrical topologies of 2-Area power System.

$\varepsilon_{0,k}(0) = \bar{\varepsilon}_k = 50\%$, while the ambient temperature is $\theta_{amb,k} = 30[°C]$, $k = 1,2$. This allows computing the baseline power according to (12), thus obtaining $p^k_{i,b}(t) = 1.68\ [MW]$. A time interval of $t = 150\ [s]$ is considered for validation purpose, where at $t = 96\ [s]$ a load increment of $1.5\ [MW]$ emulates the occurrence of a contingency within Area #1. In what follows, we firstly present the worst case scenario, where the maximum delay $\tau^\star$ is chosen as the delay stability margin preserving the stability. Then, the LHS approach (Helton and Davis, 2003) is exploited to evaluate the resilience of the controller (17) w.r.t. different $\tau^\star$ and uncertainty range of GISB parameters.

4.1 Worst Case Scenario

In this section we evaluate the robustness of the proposed distributed control in presence of network latencies both in Area #1 and Area #2. The objective is to find the delay stability margin of the overall system, i.e., the maximum admissible delay able to preserve the stability of the entire power system.

To this aim, we carried-out a simulation campaign where the heterogeneous time-varying delays τ^k_{ij} are emulated as uniformly random variables with a maximum value $\tau^\star$, which has been iteratively increased till the stability of the network has been violated. Our simulation campaign has revealed that the stability of the multi-area power system we consider is preserved till $\tau^\star = 0.2\,[s]$, which hence represents our delay stability margin.

Simulation results achieved in Area #1 in this worst case scenario are reported in Figure 3. Specifically, from Figure 3(a) it is possible to appreciate that our distributed control is able to perform the comfort recovery of all the GISBs, also after the load changing occurring at $t = 96\ [s]$, with small bounded errors during the transient phases (see Figure 3(b)). Indeed, at this time instant Δf_1 exceeds the minimum threshold (see Figure 3(c)) and, then, leader behavior switches to FSM mode according to (14). Then, from $t \in [96,120]\ [s]$, the aggregator #1 operates below its baseline power (see Figure 4(d)), thus discharging into the grid for primary frequency support. Similar

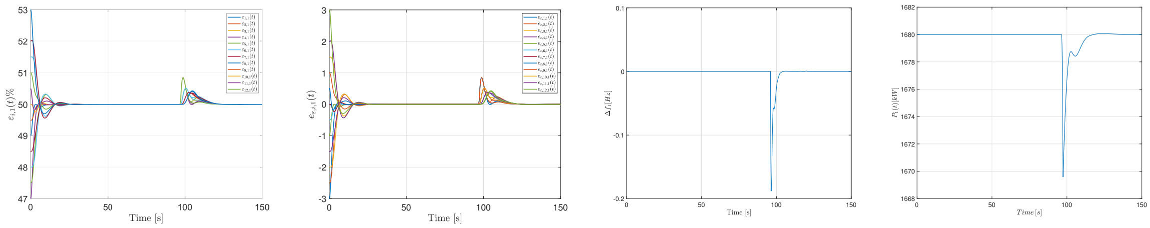

(a) (b) (c) (d)

Figure 3: Distributed frequency support control with heterogeneous time-varying delays with $\tau^{\star} = 0.2\,[s]$. Time-history of: *a)* $\varepsilon_{i,1}(t)\,[\%]$, $i \in \mathcal{V}^{c}_{N_1}$; *b)* $e_{\varepsilon,i,1}(t)\,[\%]$, $i \in \mathcal{V}^{c}_{N_1}$; *c)* $\Delta f_1(t)\,[Hz]$; *d)* $P_1(t)\,[kW]$.

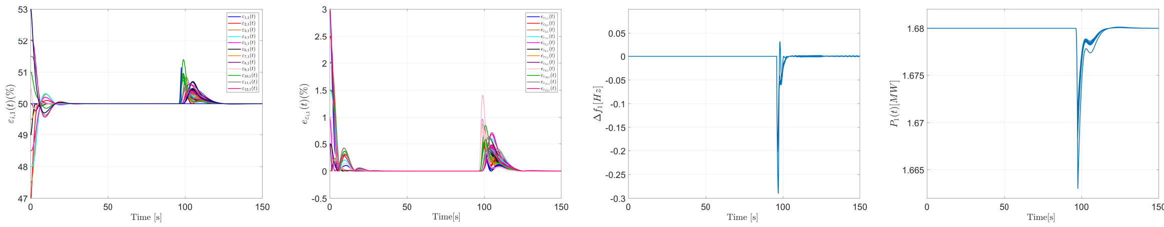

(a) (b) (c) (d)

Figure 4: Resilience analysis via LHS method in uncertain delays conditions with $\tau^{\star} = 0.1\,[s]$. Time-history of: *a)* $\varepsilon_{i,1}(t)\,[\%]$, $i \in \mathcal{V}^{c}_{N_1}$; *b)* $e_{\varepsilon,i,1}(t)\,[\%]$, $i \in \mathcal{V}^{c}_{N_1}$; *c)* $\Delta f_1(t)\,[Hz]$; *d)* $P_1(t)\,[MW]$.

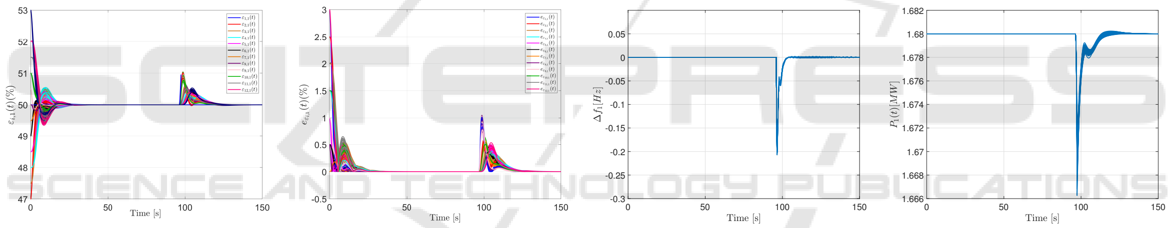

(a) (b) (c) (d)

Figure 5: Resilience analysis via LHS method in uncertain GISBs parameters conditions with $\tau^{\star} = 0.1\,[s]$. Time-history of: *a)* $\varepsilon_{i,1}(t)\,[\%]$, $i \in \mathcal{V}^{c}_{N_1}$; *b)* $e_{\varepsilon,i,1}(t)\,[\%]$, $i \in \mathcal{V}^{c}_{N_1}$; *c)* $\Delta f_1(t)\,[Hz]$; *d)* $P_1(t)\,[MW]$.

results are obtained for the Area #2 and, hence, they are omitted for the sake of brevity.

4.2 Resilience via Latin Hypercube Sampling Approach

Here we evaluate the robustness and the resilience of the proposed methodology w.r.t. delay variations as well as GISBs parameters uncertainties in both areas. Specifically, we consider two different scenarios: *a)* GISBs parameters assume their nominal values, while delays variations are considered, i.e., $\tau^{k}_{ij}(t) \in [-30\%\tau^{\star},\ +30\%\tau^{\star}]$ with $\tau^{\star} = 0.1\,[s]$; *b)* no delays variations are taken into account, while GISBs parameters uncertainties are emulated, i.e., the coefficients of the matrices $A_{i,k}$ and $B_{i,k}$ in (11) vary within the range $[-20\%,\ +20\%]$ with respect to their nominal values. To this aim, the LHS approach is exploited to confirm the resilience of the proposed control strategy under GISB uncertainties and variable communication time-delays, as well as for all the possible combinations of them. In both cases, we carried-out a number of simulations equal to 50.
Results of the two cases *a)* and *b)* are reported in Figures 4-5, which confirm the resilience of the distributed delayed controller (17) also in these uncertain conditions.

5 CONCLUSIONS

The paper has addressed the problem of frequency support for Grid-Interactive Smart Buildings (GISBs) with Thermostatically-Controlled Loads (TCLs). A distributed delayed controller has been devised in order to ensure that each GISB provides a fast frequency support, while counteracting the presence of communication delays. The delay stability margin has been found by means of an extensive simulation campaign, which has also exploited the latin hypercube sampling technique to prove the resilience of the proposed controller with respect to parameters and delays uncertainties.

REFERENCES

Andreotti, A., Caiazzo, B., Petrillo, A., and Santini, S. (2021). Distributed robust finite-time secondary control for stand-alone microgrids with time-varying communication delays. *IEEE Access*, 9:59548–59563.

Caiazzo, B., Lui, D. G., Petrillo, A., and Santini, S. (2022). Cooperative finite-time control for autonomous vehicles platoons with nonuniform v2v communication delays. *IFAC-PapersOnLine*, 55(36):145–150.

Chen, C., Wang, J., and Kishore, S. (2014). A distributed direct load control approach for large-scale residential demand response. *IEEE Transactions on Power Systems*, 29(5):2219–2228.

Duan, Q., Zeng, K., Liu, J., Du, B., and Liao, P. (2022). Aggregated control of smart building units for frequency regulation in multi-region power systems. In *2022 7th Asia Conference on Power and Electrical Engineering (ACPEE)*, pages 1209–1214. IEEE.

Ge, X., Han, Q.-L., Ding, D., Zhang, X.-M., and Ning, B. (2018). A survey on recent advances in distributed sampled-data cooperative control of multi-agent systems. *Neurocomputing*, 275:1684–1701.

Helton, J. C. and Davis, F. J. (2003). Latin hypercube sampling and the propagation of uncertainty in analyses of complex systems. *Reliability Engineering & System Safety*, 81(1):23–69.

Liu, X., Li, Y., Lin, X., Guo, J., Shi, Y., and Shen, Y. (2022). Dynamic bidding strategy for a demand response aggregator in the frequency regulation market. *Applied Energy*, 314:118998.

Wadi, M., Shobole, A., Elmasry, W., and Kucuk, I. (2024). Load frequency control in smart grids: A review of recent developments. *Renewable and Sustainable Energy Reviews*, 189:114013.

Wang, Y., Tang, Y., Xu, Y., and Xu, Y. (2019a). A distributed control scheme of thermostatically controlled loads for the building-microgrid community. *IEEE Transactions on Sustainable Energy*, 11(1):350–360.

Wang, Y., Xu, Y., and Tang, Y. (2019b). Distributed aggregation control of grid-interactive smart buildings for power system frequency support. *Applied energy*, 251:113371.

Wu, Y., Wei, Z., Weng, J., Li, X., and Deng, R. H. (2017). Resonance attacks on load frequency control of smart grids. *IEEE Transactions on Smart Grid*, 9(5):4490–4502.

Xia, M., Song, Y., and Chen, Q. (2019). Hierarchical control of thermostatically controlled loads oriented smart buildings. *Applied energy*, 254:113493.

Xiao, H., Zhang, M., Zeng, L., Wu, G., Wu, C., and Wu, C. (2023). Hierarchical control strategy of thermostatically controlled load considering multiple factors. *Energy and Buildings*, 291:113148.

Yousef, H. A., Khalfan, A.-K., Albadi, M. H., and Hosseinzadeh, N. (2014). Load frequency control of a multi-area power system: An adaptive fuzzy logic approach. *IEEE transactions on power systems*, 29(4):1822–1830.

Zhang, C., Xu, Y., Li, Z., and Dong, Z. Y. (2018). Robustly coordinated operation of a multi-energy microgrid with flexible electric and thermal loads. *IEEE Transactions on Smart Grid*, 10(3):2765–2775.

Zhao, H., Wu, Q., Huang, S., Zhang, H., Liu, Y., and Xue, Y. (2016). Hierarchical control of thermostatically controlled loads for primary frequency support. *IEEE Transactions on Smart Grid*, 9(4):2986–2998.

Zhao, N., Yue, D., Dou, C., and Shi, T. (2023). Distributed dynamic event-triggered cooperative control of multiple tcls and hess for improving frequency regulation. *IEEE Transactions on Industrial Informatics*, 20(2):1539–1549.

Zheng, L., An, Z., Xia, Q., Kandula, R. P., Saeedifard, M., Divan, D., Grijalva, S., and Abdallah, C. T. (2021). Distributed control of aggregated smart buildings for frequency regulation. In *2021 IEEE Industry Applications Society Annual Meeting (IAS)*, pages 1–8. IEEE.